Results in Physics 35 (2022) 105343

Contents lists available at ScienceDirect

Results in Physics

journal homepage: www.elsevier.com/locate/rinp

Large-amplitude electrostatic fluctuations at the Earth's magnetopause with a vortex-like distribution of hot electrons

O.R. Rufai [a,*,1], G.V. Khazanov [a,1], S.V. Singh [b,1], G.S. Lakhina [b,1]

[a] Heliophysics Division, NASA Goddard Space Flight Center, Greenbelt, MD, USA
[b] Indian Institute of Geomagnetism, New Panvel (W), Navi Mumbai 410218, India

ARTICLE INFO

Keywords:
Electrostatic solitary waves
Large-amplitude electric field
Electron acoustic waves
Vortex-like velocity distribution
Sagdeev pseudopotential technique
MMS observations

ABSTRACT

Large-amplitude electrostatic solitary waves (ESWs) associated with asymmetric magnetic reconnection at the Earth's magnetopause are studied in a four-component plasma composed of a mixture of the magnetosheath and magnetosphere plasma of a cold, warm and hot electron populations, and background ions. The species are modeled as adiabatic fluids except for the hot electrons which have a kinetic vortex-like velocity distribution. The hybrid model uses the Sagdeev pseudopotential technique to study the arbitrary amplitude ion- and electron-acoustic solitons and double layers. The numerical computations reveal that for the parameters corresponding to magnetosphere side of the ion diffusion region, only slow electron-acoustic solitons and double layer can exist. On the magnetosheath side of the ion diffusion region, only the electron-acoustic/beam solitons can exist. The electric field amplitude of the electrostatic solitary waves (ESWs) predicted by our model are consistent with the Magnetospheric Multiscale (MMS) observations.

Introduction

Electrostatic solitary waves (ESWs) are the most common interpretations for the broadband plasma turbulence observed in different regions of the magnetosphere. These structures have generally a large bipolar electric field component parallel to the background magnetic field. Recently, Magnetospheric Multiscale (MMS) spacecraft reported the observation of electrostatic solitary waves (ESWs) associated with asymmetric magnetic reconnection at the Earth's magnetopause [1,2]. The magnetic reconnection process generating ESWs occurs between the low-density plasma in the magnetosphere and the high-density plasma in the magnetosheath. Such electrostatic structures have been reported earlier in the auroral region by S3-3 [3], Viking [4], and FAST [5] satellites, in the polar cup boundary layer by POLAR satellite [6], in the plasma sheet boundary layer by GEOTAIL satellite [7], in the Earth's magnetosheath [8–10] and magnetopause [11] by Cluster spacecraft, in the Earth's radiation belts [12] by the Van Allen Probes.

Theoretically, electrostatic solitary waves (ESWs) with symmetric electric field structures were often identified either as kinetic BGK electron/ion phase space holes generated by a beam, two-stream, or kinetic Buneman instability [13–18] or electron/ion acoustic solitons and double layers having symmetric/asymmetric electric fields which can be generated by fluid electron/ion beam instability [19–28]. In space and astrophysical plasmas, the symmetric ESWs associated with electron/ion beam mode have been studied with multi-fluid dynamic theory by several authors [29–39]. Lakhina et al. [33] studied large-amplitude ion- and electron-acoustic waves in an unmagnetized multi-fluid plasma system consisting of a cold background electrons, two counter-streaming electron beams and ions using the Sagdeev pseudo-potential technique. Based on the plasma parameters considered, they found three types of solitary structures, namely, ion acoustic solitons having positive potentials, slow electron acoustic solitons having negative potentials and fast electron acoustic solitons and double layers which can either be positive or negative potentials depending on the core electron density. In line with the Van Allen Probes observations, Vasko et al. [40] investigated the nature of the asymmetric ESWs in terms of electron acoustic solitons and double layers in a suprathermal hot electron plasma using the Korteweg–de Vries (KdV) technique. In a later paper, Vasko et al. [41] studied the mechanism of generating nonlinear electrostatic steepening whistler waves in a classical hydrodynamic fluid model composed of two-temperature electron plasma with κ-distribution electron. In a fluid plasma system consisting of a two-temperature (cold and hot) electron populations, Dillard et al. [42] derived the modified KdV equation for the asymmetric electrostatic solitary waves (ESWs) in terms of electron acoustic solitons and double layers (shock) in the Earth's inner magnetosphere.

* Corresponding author.
E-mail address: odutayoraji.rufai@nasa.gov (O.R. Rufai).
[1] All authors work together.

https://doi.org/10.1016/j.rinp.2022.105343
Received 5 June 2021; Received in revised form 6 November 2021; Accepted 13 February 2022
Available online 26 February 2022

Several MMS observations have indicated that the energy distribution of the hot electron species trapped in the phase space holes deviated from the standard Boltzmann-Maxwell equilibrium to exhibit vortex-like structures during the magnetic reconnection in the diffusion region of the magnetopause [1,2,43] and magnetotail [44–49]. The established kinetic vortex-like velocity distribution function for trapped energetic particles derived from the Vlasov equation is given by Schamel [18,50]

$$f(v) = \frac{1}{\sqrt{2\pi}} e^{-\frac{1}{2}(\beta(v^2-2\phi))}, \quad |v| \leq \sqrt{2\phi} \tag{1}$$

where v is the velocity normalized by the hot electron thermal speed $v_{th} = \sqrt{T_h/m_e}$, ϕ is the electric potential normalized by T_h/e, T_h and m_e are the equilibrium temperature and mass respectively. Further, β controls the trapping of electrons and shape of the distribution function. For $\beta = 1(0)$, Eq. (1) represents a shifted Maxwellian and a flat top distribution respectively. For $\beta < 0$, Eq. (1) represents the trapped electron distribution with a hole in the phase space. The early theoretical kinetic BGK analysis of Schamel [18] established the fundamental characteristics of the trapped parameter β on the finite amplitude electrostatic structures. Low-frequency ion acoustic waves have been studied in superthermal plasmas using the Schamel equation [51,52]. These analysis were later adopted in fluid dynamic theory by Mamun et al. [53–55] to study the effects of trapped particles on finite amplitude dust/electron-acoustic solitary waves using the Korteweg–de Vries (KdV) approach of reductive perturbation technique. Using the Sagdeev pseudo-potential technique, Mushtaq et al. [56] studied the large amplitude ion-acoustic solitary waves in a multi-fluid ions plasma with trapped electrons.

Recently, Mbuli et al. [35,36], studied the characteristics of arbitrary amplitude slow and fast electron acoustic solitons and double layers in a four-component plasma system consisting of cold, warm and hot electrons, and ions, where all species are treated as adiabatic fluid. In this paper, we modified the model of Mbuli et al. [35,36] to assume a kinetic vortex-like velocity distribution for the hot electron species while cold and warm electrons, and ions are treated as adiabatic fluids. This model appears capable of simulating the MMS large-amplitude electrostatic solitary waves associated with asymmetric magnetic reconnection at the Earths magnetopause [1] in terms of low-frequency (ion acoustic) and high-frequency (electron acoustic) solitons and double layers. More recently, Rufai et al. [57] studied the existence of nonlinear electron acoustic solitons in the electron diffusion region with two temperature electrons composed of a hot trapped electrons having vortex-like velocity distribution and a warm fluid adiabatic electrons using the MMS parameters. They employed the reductive perturbation technique which leads to a modified Korteweg–de Vries (mKdV) equation of small but finite amplitude electron acoustic waves.

Moreover, for MMS large amplitude ESWs studies, we extend the work of Rufai et al. [57] by introducing additional adiabatic electron species, i.e., a cold electron beam of the magnetosphere plasma component in the system. In Section “Theoretical model”, the theoretical model and derivation of the Sagdeev pseudopotential for the localized nonlinear structures are presented. The numerical results are discussed in Section “Numerical Results”. A conclusion of the findings is given in Section “Conclusion”.

Theoretical model

Based on the MMS observations reported by Ergun et al. [1], we consider a four-component, homogeneous, collisionless and unmagnetized magnetopause plasma system composed of a cold magnetospheric electrons (N_c, T_c, V_{dc}) propagating parallel to the magnetic field with respect to the warm magnetosheath electrons (N_w, T_w, V_{dw}) streaming antiparallel, hot electrons (N_h, T_h), and background ions (N_i, T_i), where, N_j, T_j, V_{dj} represents the equilibrium values of density, temperature and drift velocity of the species j, and $j = c, w, h$ and i for the cold, warm, hot electrons, and ions, respectively. The hot electrons are assumed to be following the kinetic vortex-like velocity distribution given in Eq. (1) and their number density can be expressed as [18,50]

$$n_h = n_{h0}[I(\phi)] + n_{h0}|\beta|^{-1/2} \begin{cases} \exp(\beta\phi)\,\mathrm{erf}(\sqrt{\beta\phi}) & \beta \geq 0 \\ \frac{2}{\sqrt{\pi}} W_D(\sqrt{-\beta\phi}) & \beta < 0 \end{cases} \tag{2}$$

where

$$I(\phi) = (1 - \mathrm{erf}\,(\sqrt{\phi}))e^{\phi},$$

the error, $\mathrm{erf}(\phi)$ and Dawson, $W_D(\phi)$ function is defined by

$$\mathrm{erf}(\phi) = \frac{2}{\sqrt{\pi}} \int_0^{\phi} e^{-t} dt, \quad W_D(\phi) = e^{(-\phi^2)} \int_0^{\phi} e^{t^2} dt.$$

Here, ϕ is the electric potential. In the limit $\beta \to 1$, the Boltzmann-Maxwell equilibrium of hot electron can be recovered, $\beta > 0$ ($\beta < 0$) represents a vortex-like distribution. Thus, the case $\beta > 0$ in Eq. (2) satisfied the arbitrary large amplitude perturbation for the trapped hot electrons and the normalized density can be expressed as

$$n_h = n_{h0}\left(e^{\phi}\,\mathrm{erf}\,c(\sqrt{\phi}) + \frac{e^{\beta\phi}}{\sqrt{\beta}}\,\mathrm{erf}(\sqrt{\beta\phi})\right), \tag{3}$$

where the complementary error function $\mathrm{erf}\,c(\phi) = 1 - \mathrm{erf}(\phi)$. Whereas, in small amplitude limit, the normalized hot electron density can be expressed as

$$n_h = n_{h0}\left(1 + \phi - \frac{4(1-\beta)}{3\sqrt{\pi}}(\phi)^{3/2} + \frac{(\phi)^2}{2} + \cdots.\right). \tag{4}$$

While, the cold magnetospheric, warm magnetosheath electrons and ions are assumed to be mobile and they are governed by the following adiabatic fluid equations [21]: the continuity equation

$$\frac{\partial n_j}{\partial t} + \frac{\partial (n_j v_j)}{\partial x} = 0, \tag{5}$$

the momentum equation

$$\frac{\partial v_j}{\partial t} + v_j \frac{\partial v_j}{\partial x} + \frac{1}{\mu_j n_j}\frac{\partial P_j}{\partial x} + \frac{Z_j}{\mu_j}\frac{\partial \phi}{\partial x} = 0, \tag{6}$$

the equation of state

$$\frac{\partial P_j}{\partial t} + v_j \frac{\partial P_j}{\partial x} + 3P_j \frac{\partial v_j}{\partial x} = 0, \tag{7}$$

the Poisson equation

$$\frac{\partial^2 \phi}{\partial x^2} = -\sum_j Z_j n_j. \tag{8}$$

Here, n_j, v_j, P_j, and $\mu_j = m_j/m_e$, density, velocity, pressure, and mass ratio of the jth species and the ions, $Z_j(= -1(+1))$ for electrons (ions), respectively. Moreover, the number densities are normalized by the total equilibrium plasma density $n_{j0} = N_j/N_0$ such that $n_{c0} + n_{w0} + n_{h0} = n_{i0} = 1$. Keeping in mind the application to magnetospheric observations where hot electrons are observed, Eqs. (1)–(8) are normalized in the following manner:temperature are normalized by the hot electron temperature, T_h, time is normalized by the inverse of total electron plasma frequency $\omega_{pe}^{-1} = \sqrt{m_e/4\pi N_0 e^2}$, velocities by the electron thermal velocity $v_{th} = (T_h/m_e)^{1/2}$, spatial lengths by $\lambda_{dh} = (T_h/4\pi N_0 e^2)^{1/2}$, electrostatic potential ϕ is normalized by T_h/e, and the thermal pressures P_j by $N_0 T_h$. For magnetosheath case as there are no observations of hot electrons, Eqs. (5)–(8) remain valid, however, the normalizations used are as follows: the temperatures are normalized by the ion temperature T_i, time is normalized by the inverse of ion plasma frequency, $\omega_{pi}^{-1} = (4\pi N_0 e^2/m_i)^{-1/2}$, velocities by the ion thermal velocity $v_{ti} = (T_i/m_i)^{1/2}$, spatial lengths by $\lambda_{di} = (T_i/4\pi N_0 e^2)^{1/2}$, electrostatic potential ϕ is normalized by T_i/e, and the thermal pressures P_j by $N_0 T_i$. Here $\mu_j = m_j/m_i$. For the case of a one dimensional system, the adiabatic index $\gamma = 3$ is justified for all the mobile species (e.g. cold, warm electrons and ions) in the equation of state given by Eq. (7). Analytically, we present the case of ion diffusion region on the magnetospheric side.

We employ the Sagdeev pseudo-potential technique for the arbitrary amplitude electrostatic solitary waves, which conserve the full complexity of the localized nonlinear structures. The analysis involved the transformation of all the dependent variables in Eqs. (5)–(7) to a single independent variable in a moving frame of reference, i.e.

$$\xi = x - Mt \tag{9}$$

where $M = V/v_{th}$ (V is the wave phase speed).

Using Eq. (9) in Eq. (5)–(8) and solving for the perturbed densities of cold, warm electrons and ions and substituting these expressions into the Poisson equation, and assuming appropriate boundary conditions for the localized structures such as, $n_j \to n_{j0}$, $v_j \to v_{dj}$, $\phi = d\phi/d\xi \to 0$, $\mathrm{erf}(\sqrt{\beta\phi}) \to 0$, $e^{\phi}\,\mathrm{erf}\,c(\sqrt{\phi}) \to 1$, and $P_j \to P_{j0} \sim n_{j0}T_j/T_h$ at $\xi \to \pm\infty$, we obtain the following energy integral

$$\frac{1}{2}\left(\frac{d\phi}{d\xi}\right)^2 + S(\phi, M) = 0, \tag{10}$$

where the Sagdeev potential $S(\phi, M)$ is written as

$$S(\phi, M) = n_{h0}\left(1 - \left(e^{\phi}\,\mathrm{erf}\,c(\sqrt{\phi}) + \frac{2\sqrt{\phi}}{\sqrt{\pi}}\left(1 - \frac{1}{\beta}\right) + \frac{e^{\beta\phi}}{\beta\sqrt{|\beta|}}\,\mathrm{erf}(\sqrt{\beta\phi})\right)\right) + \sum_j \frac{n_{j0}\mu_j}{6\sqrt{3\delta_j}}\left[\left[\left((M - v_{dj}) + \sqrt{3\delta_j}\right)^3 - \left(\sqrt{\left((M - v_{dj}) + \sqrt{3\delta_j}\right)^2 - \frac{2Z_j\phi}{\mu_j}}\right)^3\right] \pm \left[\left((M - v_{dj}) - \sqrt{3\delta_j}\right)^3 - \left(\sqrt{\left((M - v_{dj}) - \sqrt{3\delta_j}\right)^2 - \frac{2Z_j\phi}{\mu_j}}\right)^3\right]\right], \tag{11}$$

where $\delta_j = \frac{P_{j0}}{n_{j0}\mu_j}$. Eq. (10) describes the motion of a pseudo-particle of unit mass in a Sagdeev pseudo-potential $S(\phi, M)$ where ϕ and ξ are the displacement from the equilibrium and time, respectively. Moreover, the hot electron contribution in Eq. (11) corresponding to a distribution of trapped electrons is similar to Mushtaq et al. [56] for the case of low-frequency ion-acoustic waves in two ions plasma.

The criteria for solitary wave solutions are: $S(\phi, M)$ satisfies the following conditions: $S(\phi, M) = 0$, $dS(\phi, M)/d\phi = 0$, and $d^2S(\phi, M)/d\phi^2 < 0$ at $\phi = 0$; $S(\phi, M) = 0$ at $\phi = \phi_m$ and $S(\phi, M) < 0$ for $0 < |\phi| < |\phi_m|$, where ϕ_m is the maximum potential. For double layer (DL) solutions, one more additional condition should be satisfied, namely, $dS(\phi, M)/d\phi = 0$ at $\phi = \phi_m$ [21,32,58].

One can check that both $S(\phi, M)$ and its first derivative with respect to ϕ vanish at $\phi = 0$. For the Mach number domain, the condition $d^2S(\phi, M)/d\phi^2 < 0$ at $\phi = 0$ is satisfied provided $M > M_0$, where M_0 (critical Mach number) satisfies the following equation, i.e.,

$$\frac{d^2S(\phi, M)}{d\phi^2}\Big|_{\phi=0} = f(M_0) \equiv \sum_j \frac{Z_j^2 n_{j0}}{\mu_j\left((M_0 - v_{dj})^2 - 3\delta_j\right)} - n_{h0} = 0. \tag{12}$$

Numerically, Eq. (12) yields 6 roots as the critical Mach numbers (M_0) but only three are positive roots with physical interpretations, which correspond to the three nonlinear modes, namely, ion acoustic, slow electron acoustic and fast electron acoustic modes. Moreover, for a given set of plasma parameters, any one, two or all the three modes can satisfy the solitary wave conditions given above.

Numerical results

We now apply our results to the MMS spacecraft observations in the ion diffusion region of the Earth's magnetopause using the parameters

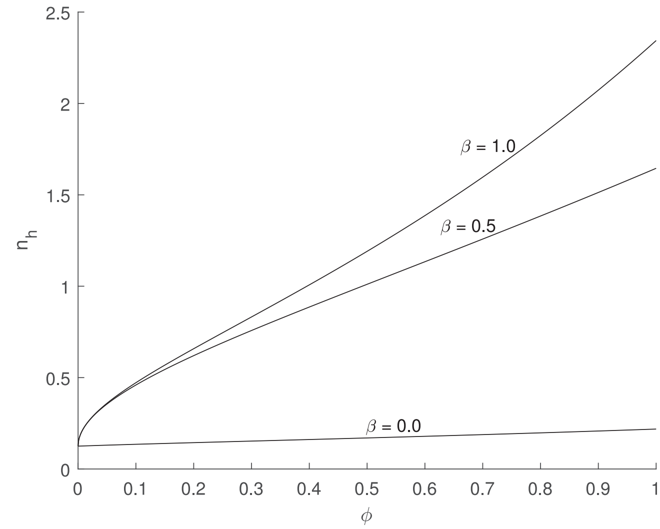

Fig. 1. Variation of normalized hot electrons density, n_h vs. normalized electrostatic potential ϕ.

from Ergun et al. [1]. On the magnetospheric side of the diffusion region, the plasma parameters are as follows: Cold electrons; densities, $N_c = 2$ cm^{-3}, drift velocity, $V_{dc} = 0.25\ v_{thew}$, temperatures, $T_c = 1$ eV. Warm electrons; densities, $N_w = 1.5$ cm^{-3}, drift velocity, $V_{dw} = 0.25\ v_{thew}$ (v_{thew} is the warm electron thermal speed), temperatures, $T_w = 100$ eV. Hot electrons; densities, $N_h = 0.5$ cm^{-3}, temperatures, $T_h = 1$ keV; and Ions: temperatures, $T_i = 1$ eV. Based on the above parameters, the normalized plasma parameters for the computations are as follows: $n_{c0} = 0.5$, $n_{w0} = 0.375$, $n_{h0} = 0.125$, and $v_{dc} = -v_{dw} = 0.079$. The above mentioned plasma parameters are used through out the computations in each figure, otherwise specified wherever variations are carried out.

The characteristics of the normalized trapped hot electrons density (n_h) calculated from Eq. (3) are displayed in Fig. 1 for different values of β for $n_{h0} = 0.125$. It is observed that the arbitrary amplitude perturbation for the trapped hot electrons density grows with β and the curve $\beta = 1.0(0.0)$ corresponds to Boltzmann (flat top) hot electrons distribution.

Fig. 2 shows the existence domain as a function of equilibrium hot electron density n_{h0} for the only possible type of electrostatic solitary mode, namely, slow electron acoustic mode. It is important to mention that the corresponding low-frequency ion acoustic solitary structures are not found. Moreover, the fast electron acoustic mode appears unphysical as its velocity exceeds the hot electron thermal speed. These Mach number ranges occur in the highest Mach number domain $M_0 > 1$. The critical Mach numbers M_0 for the slow electron acoustic mode are found between $0.393 \leq M_0 \leq 0.422$ for $n_{h0} = 0.1 - 0.3$ and these soliton velocities lie between cold and warm electron thermal speeds, i.e., $\sqrt{3v_{tc}} < M_0 < \sqrt{3v_{tw}}$. The critical Mach number, M_0 for slow electron acoustic solitons increases with increase in number density of hot electrons. The upper $M_{max}(M_{DL})$ and critical M_0 Mach number range can be found to exist only at the positive potential region for the slow electron-acoustic modes of the nonlinear electrostatic solitary structures which are plotted in Fig. 2(a). In Fig. 2(a), positive potential slow electron acoustic solitons which have upper bound due to the formation of a double layer (M_{DL}) are found to exist in RI (n_{h0} : 0.1 – 0.19). In Region II (n_{h0} : 0.2 – 0.3) also shows the presence of positive potential solitons, no double layers are found. Beyond $n_{h0} = 0.19$, we noted that the slow electron acoustic solitons exhibit a constant upper Mach number value, (M_{max}) of $M = 0.468$ in RII. Fig. 2(b) shows the plot for the upper Mach number against the trapped parameter β. The increase of the trapped parameter β decrease the upper Mach numbers and $\beta = 1.0$ corresponding to the Boltzmann-Maxwellian equilibrium.

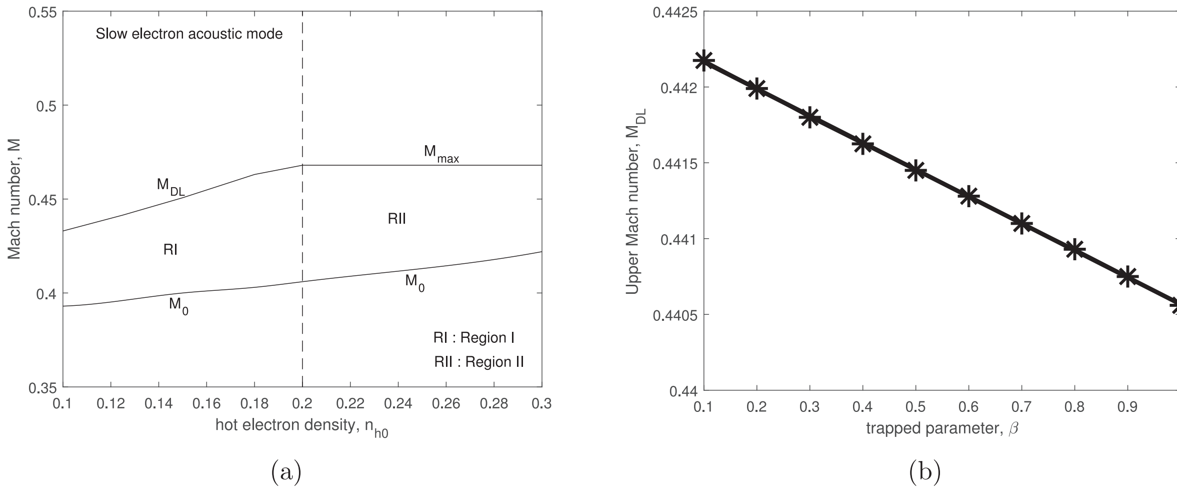

Fig. 2. (a) Existence domain for the electrostatic structures represented by a plot of the range of Mach number against the normalized hot electron number density n_{h0} for $\beta = 0.5$ and other fixed parameters are $n_{c0} = 0.5$, $v_{dc} = -v_{dw} = 0.079$, $m_i/m_e = 1836$, $T_c = T_i = 1$ eV, $T_w = 100$ eV, $T_h = 1$ keV. There are two distinct existence regions for the slow electron acoustic waves: RI has positive potential solitons which are bounded above by the formation of a double layer (M_{DL}); Region II has positive potential solitons with an upper limit M_{max}. (b) The plot for the upper Mach number against the trapped parameter, β for the same fixed parameters of Fig. 2(a).

Table 1
Properties of slow electron acoustic solitons (S) and double layers (DL) such as the velocity (V), electric field (E), width (W) and pulse duration (τ) in the magnetospheric side of the diffusion region as functions of the cold electron density $n_{c0} = 0.5$, $\beta = 0.5$, $v_{dc} = -v_{dw} = 0.079$, $m_i/m_e = 1836$, $T_c = T_i = 1$ eV, $T_w = 100$ eV, $T_h = 1$ keV. The corresponding magnetosphere total electron density, $N_0 = 4.0$ cm^{-3} [1] yields Debye length, $\lambda_{dh} = 117.54$ m.

n_{h0}, n_{w0}	Polarity	V (10^2 km s^{-1})	E (mV m^{-1})	W (m)	τ (ms)
0.1, 0.4	$+ve(S/DL)$	52.11–57.42	0.11–100	1916–911	0.37–0.16
0.125, 0.375	$+ve(S/DL)$	52.64–58.54	0.50–120	1200–832	0.23–0.14
0.15, 0.35	$+ve(S/DL)$	53.31–59.76	1.53–123	811–893	0.15–0.14
0.2, 0.3	$+ve(S)$	54.50–62.06	2.72–110	654–733	0.12–0.12
0.25, 0.25	$+ve(S)$	55.82–62.06	3.94–77	552–449	0.1–0.07
0.3, 0.2	$+ve(S)$	57.28–62.06	5.00–47	477–383	0.08–0.06

In addition, the nonlinear structures can exist only in the positive potential region. It is important to note that the trapped parameter β does not have any effect on the critical Mach number as is obvious from the expression (12).

We further show the Sagdeev potential profiles $S(\phi, M)$ and the corresponding normalized electrostatic potential ϕ of the slow electron acoustic structures, which are all having positive polarities for the fixed plasma parameters, $n_{c0} = 0.5$, $n_{w0} = 0.375$, $n_{h0} = 0.125$, $\beta = 0.5$, $v_{dc} = -v_{dw} = 0.079$, $m_i/m_e = 1836$, $T_c = T_i = 1$ eV, $T_w = 100$ eV, $T_h = 1$ keV. For these fixed plasma parameters, the Sagdeev potential (Figs. 3a and 3c) and normalized electrostatic soliton profiles (Fig. 3b) for the slow electron acoustic structures which are limited by the formation of a double layers are shown in Fig. 3. In Fig. 3a, the double layer solution corresponds to mach number, $M = 0.44145$. In this case both the electrostatic potential amplitude and width increases with an increase in M as can be seen from soliton potential profiles in Fig. 3b. In Fig. 3c, sagdeev potential is plotted for different values of β for M=0.441 and other plasma parameters being the same as in Figs. 3a and 3b. From Fig. 3c, it is seen that soliton amplitude increases with increase in β till a double layer (DL) is reached at $\beta = 0.75$. Beyond this value of β, the solitons/DLs solutions do not exist as evident from the curve for $\beta = 1$ corresponding to Maxwell–Boltzmann equilibrium of hot electrons.

In Table 1, the properties of the nonlinear electrostatic solitons and double layers in terms of unnormalized electric field amplitude, E, velocities, V, width, W, and time duration, $\tau = W/V$ are presented. For the magnetosphere plasma component, Table 1, shows the property of the slow electron acoustic solitons and double layers as a function of hot and warm electron number density, n_{h0} and n_{w0} respectively.

It is seen from Table 1 that with n_{h0} increasing, the width and pulse duration of the slow electron acoustic waves decreases whereas soliton velocity increases along with lower values of the electric field. The maximum soliton velocity reaches a plateau for $n_{h0} > 0.2$. Further, maximum amplitude increase upto $n_{h0} = 0.15$ and thereafter it decreases. For the observed value of $n_{h0} = 0.125$, the model predicts a maximum electric field of 120 mV/m for the slow electron acoustic waves. The amplitude of the electrostatic solitary waves observed by MMS spacecraft at the Earth's magnetopause associated with the asymmetric parallel electric field structures is of the order of ≥100 mV/m [1]. Thus, electric amplitude predicted by our model matches well with the observations.

We shall now discuss the case corresponding to the magnetosheath side of the ion diffusion region where the hot electrons population is absent, i.e., $n_{h0} = 0$, and the cold magnetospheric electron beam penetrates into the magnetosheath. On the magnetosheath side of the diffusion region [1], the plasma parameters are as follows: Cold electrons; densities, $N_c = 0.2$ cm^{-3}, drift velocity, $V_{dc} = 2.36\ v_{thew}$, temperatures, $T_c = 0.5$ eV. Warm electrons; densities, $N_w = 30$ cm^{-3}, drift velocity, $V_{dw} = 0$, temperatures, $T_w = 100$ eV, and Ions: temperatures, $T_i = 100$ eV. In this case, as there are only two electron species, i.e., warm magnetosheath electrons and cold electron beam from the magnetosphere, only the electron acoustic/beam modes are generated as found by Ergun et al. [1]. Following normalized plasma parameters are obtained from the above mentioned parameters, i.e., $n_{c0} = 0.007$, $n_{w0} = 0.993$, $v_{dc} = 101$, $v_{dw} = 0$, $m_e/m_i = 1/1836$. Once again, low-frequency ion acoustic mode does not exist. The Sagdeev potential curves plotted in Fig. 4a represents the electron-acoustic/beam mode with $M_{max} = 2.75$ as the upper bound of the soliton structures. The positive potential soliton amplitude increases with the Mach number M, but its width decreases as can be seen from the normalized electrostatic soliton potential profiles in Fig. 4b. Their corresponding bipolar parallel electric field profiles are present in Fig. 4c. Here the Mach

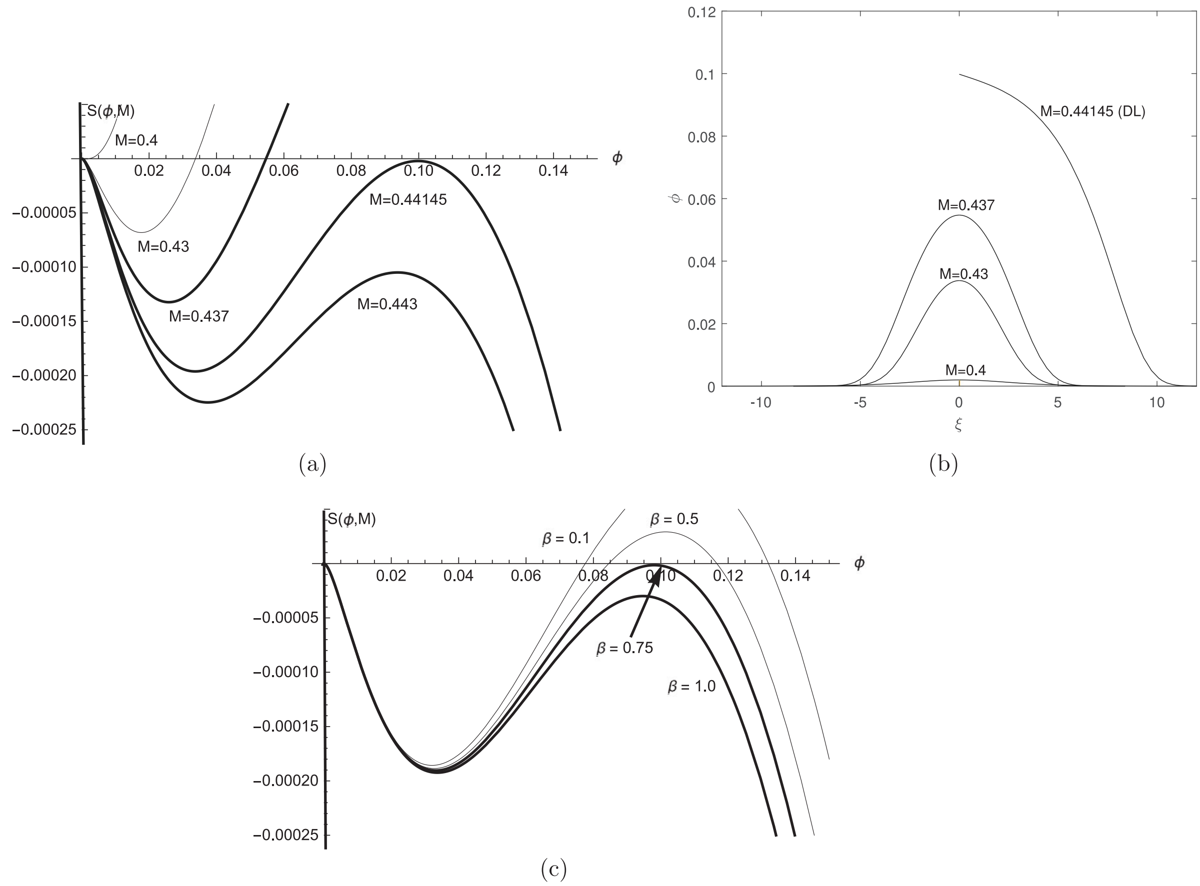

Fig. 3. (a) Sagdeev potential profiles for the slow electron-acoustic waves for $n_{c0} = 0.5$, $n_{w0} = 0.375$, $n_{h0} = 0.125$, $\beta = 0.5$, $v_{dc} = -v_{dw} = 0.079$, $m_i/m_e = 1836$, $T_c = T_i = 1$ eV, $T_w = 100$ eV, $T_h = 1$ keV, (b) The corresponding solitons and double layer profiles, (c) Sagdeev potential profiles for different values of β for $M = 0.441$.

Table 2
Properties of beam/electron acoustic solitons (S) such as the velocity (V), electric field (E), width (W) and pulse duration (τ) in the magnetosheath side of the diffusion region as functions of the Mach number M for $v_{dc} = 101$, $m_e/m_i = 1/1836$, $T_c = 0.5$ eV, $T_w = T_i = 100$ eV. The corresponding magnetosheath total electron density, $N_0 = 30.2$ cm^{-3} [1] yields Debye length, $\lambda_{di} = 13.5$ m.

M	Polarity	V (10^2 km s^{-1})	E (m Vm^{-1})	W (m)	τ (μs)
2.46	$+ve(S)$	2.36	0.81	1000	4.23
2.60	$+ve(S)$	2.50	157.60	167	0.67
2.70	$+ve(S)$	2.60	356.70	123	0.47
2.75	$+ve(S)$	2.64	468.40	111	0.42

number is defined with respect to ion thermal speed, i.e., $M = V/v_{ti}$. The properties of electron acoustic/beam mode are given in Table 2.

Table 2 shows the properties of the positive potential beam/electron acoustic soliton structures generated in the magnetosheath side of the diffusion region where the hot electron population is absent. For the fixed plasma parameters as in Fig. 4, the electric amplitude and wave velocity increase with the increase in the Mach number M. The soliton width, as well as pulse duration, decreases with the Mach number M. Here in the magnetosheath side of the ion diffusion region, the model predicts a maximum electric field of ~470 mV/m for the electron-acoustic/beam mode. This model also agrees with the observed electric field amplitude of the order of ≥100 mV/m reported by Ergun et al. [1] at the Earth's magnetopause.

Conclusion

Theoretically, we have explored the existence of electrostatic solitary waves (ESWs) associated with asymmetric magnetic reconnection at the Earth's magnetopause using a hybrid of fluid dynamic model and kinetic vortex-like velocity distribution. The results of the findings are applied to the magnetospheric as well as magnetosheath sides of the ion diffusion region. The plasma parameters are determined from the observations of ESWs by MMS spacecraft [1]. For the plasma parameters on the magnetospheric side of the diffusion region, the model supports the existence of slow electron acoustic solitons and double layers in the presence of hot magnetosheath electrons having vortex-like distribution. These nonlinear structures have positive polarities. However, on the magnetosheath side of the diffusion region where the hot electrons are absent and cold magnetospheric beam electrons are present in the magnetosheath, only beam/electron acoustic solitons are found to exist. The theoretical model for the electrostatic solitary waves (ESWs) presented here is for arbitrary large amplitude fluctuations using the Sagdeev pseudopotential technique. So, the characteristics and properties of the nonlinear soliton and double layer structures generated will depend on the plasma parameters considered.

The properties of the soliton and double layer structures predicted by our plasma model are in good agreement with the properties of the large-amplitude electrostatic solitary waves (ESWs) associated with asymmetric electric field structures observed by Magnetospheric Multiscale (MMS) at the Earth's magnetopause. The electric field amplitude obtained from our model (slow electron-acoustic and electron-acoustic/beam modes) agrees with the MMS observations. We are unable to compare our predictions of the polarity, pulse duration and widths with the observations as these are not provided in [1].

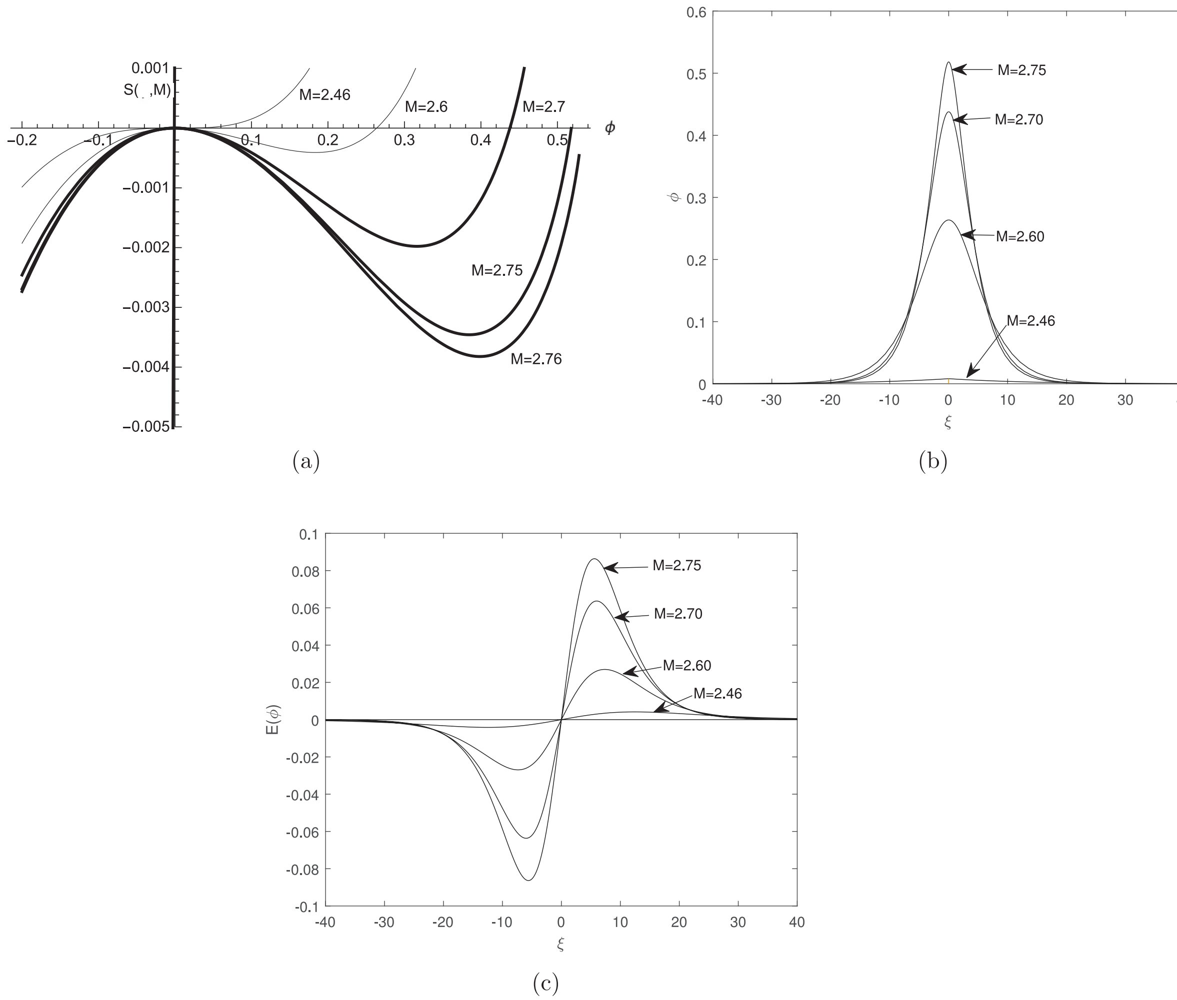

Fig. 4. (a) Sagdeev potential profiles for the electron-acoustic solitons in the absence of hot electron population in the magnetosheath, and for $n_{c0} = 0.007$, $n_{w0} = 0.993$, $v_{dc} = 101$, $v_{dw} = 0$, $m_e/m_i = 1/1836$, $T_c = 0.5$ eV, $T_w = T_i = 100$ eV, (b) the corresponding compressive electrostatic solitons, and (c) corresponding bipolar parallel electric field structures. It should be noted that the Mach number is defined with respect to thermal speed, $M = V/v_{ti}$.

Declaration of competing interest

The authors declare that they have no known competing financial interests or personal relationships that could have appeared to influence the work reported in this paper.

Acknowledgments

ORR would like to acknowledge the financial support of the NASA/USRA Postdoctoral Fellowship Program (NPFP), USA. GSL thanks the Indian National Science Academy, New Delhi, India for the support under the INSA-Honorary Scientist Scheme. Data is available through Ergun et al. [1]. MMS data are also open to the public (https://lasp.colorado.edu/mms/sdc/public/).

References

[1] Ergun RE, Holmes JC, Goodrich KA, Wilder FD, Stawarz JE, Eriksson S, et al. Magnetospheric multiscale observations of large-amplitude, parallel, electrostatic waves associated with magnetic reconnection at the magnetopause. Geophys Res Lett 2016;43:5626–34. http://dx.doi.org/10.1002/2016GL068992.

[2] Graham DB, Vaivads A, Khotyaintsev Yu V, Andre M, Contel O Le, et al. Large-amplitude high-frequency waves at Earth's magnetopause. J Geophys Res: Space Phys 2018;123:2630–57. http://dx.doi.org/10.1002/2017JA025034.

[3] Temerin M, Cerny K, Lotko W, F.S Mozer. Observations of double layers and solitary waves in the auroral plasma. Phys Rev Lett 1982;48:1175. http://dx.doi.org/10.1103/PhysRevLett.48.1175.

[4] Bostrom R, Holback B, Holmgren G. Solitary structures in the magnetospheric plasma observed by viking. Phys Scr 1989;39:782–6. http://dx.doi.org/10.1088/0031-8949/39/6/022/pdf.

[5] Ergun RE, Carlson CW, McFadden JP, Mozer FS, Delory GT, Peria W, et al. Fast satellite observations of electric field structures in the auroral zone. Geophys Res Lett 1998;25:2041. http://dx.doi.org/10.1029/98GL00636.

[6] Tsurutani BT, Arballo JK, Lakhina GS, Ho CM, Buti B, Pickett JS, et al. Plasma waves in the dayside polar cap boundary layer: Bipolar and monopolar electric pulses and whistler mode waves. Geophys Res Lett 1998;25(22):4117–20. http://dx.doi.org/10.1029/1998GL900114.

[7] Matsumoto H, Kojima H, Miyatake T, Omura Y, Okada YM, Nagano I, et al. Electrostatic solitary waves (ESW) in the magnetotail: Ben wave forms observed by GEOTAIL. Geophys Res Lett 1994;21:2915–8. http://dx.doi.org/10.1029/94GL01284.

[8] Pickett JS, Menietti JD, Gurnett DA, Tsurutani B, Kintner P, Klatt E, et al. Solitary potential structures observed in the magnetosheath by the cluster spacecraft. Nonlinear Processes Geophys 2003;10(2003):3–11. http://dx.doi.org/10.5194/npg-10-3-2003.

[9] Pickett JS, Chen L-J, Kahler SW, Santolik O, Gurnett DA, Tsurutani BT, Balogh A. Isolated electrostatic structures observed throughout the cluster orbit: Relationship to magnetic field strength. Ann Geophys 2004;22:2515–23. http://dx.doi.org/10.5194/angeo-22-2515-2004.

[10] Pickett JS, Chen L-J, Kahler SW, Santolik O, Goldstein ML, Lavraud B, et al. On the generation of solitary waves observed by cluster in the near-earth magnetosheath. Nonlinear Pro Geophys 2005;12(2):181–93. http://dx.doi.org/10.5194/npg-12-181-2005.

[11] Graham DB, Khotyaintsev Yu V, Vaivads A, Andre M. Electrostatic solitary waves with distinct speeds associated with asymmetric reconnection. Geophys Res Lett 2015;42:215224. http://dx.doi.org/10.1002/2014GL062538.

[12] Mozer FS, Agapitov OV, Artemyev A, Drake JF, Krasnoselskikh V, Lejosne S, et al. Time domain structures: What and where they are, what they do, and how

they are made. Geophys Res Lett 2015;42:3627–38. http://dx.doi.org/10.1002/2015GL063946.

[13] Bernstein IB, Greene JM, Kruskal MD. Exact nonlinear plasma oscillations. Phys Rev 1957;108:546. http://dx.doi.org/10.1103/PhysRev.108.546.

[14] Hutchinson IH. Electron holes in phase space: What they are and why they matter. Phys Plasmas 2017;24(5):055601, https://aip.scitation.org/doi/10.1063/1.4976854.

[15] Muschietti L, Ergun RE, Roth I, Carlson CW. Phase-space electron holes along magnetic field lines. Geophys Res Lett 1999;26:1093. http://dx.doi.org/10.1029/1999GL900207.

[16] Muschietti L, Ergun RE, Roth I, Carlson CW. Correction to phase-space electron holes along magnetic field lines. Geophys Res Lett 1999;26:1689. http://dx.doi.org/10.1029/1999GL900302.

[17] Omura Y, Kojima H, Matsumoto H. Computer simulation of electrostatic solitary waves: A nonlinear model of broadband electrostatic noise. Geophys Res Lett 1994;21:2923–6. http://dx.doi.org/10.1029/94GL01605.

[18] Schamel H. Stationary solitary, snoidal and sinusoidal ion acoustic waves. Plasma Phys 1972;14:905, https://iopscience.iop.org/article/10.1088/0032-1028/14/10/002.

[19] Berthomier M, Pottelette R, Malingre M. Solitary waves and weak double layers in a two-electron temperature auroral plasma. J Geophys Res 1998;103(A3):4261–70. http://dx.doi.org/10.1029/97JA00338.

[20] Kakad AP, Singh SV, Reddy RV, Lakhina GS, Tagare SG, Verheest F. Generation mechanism for electron acoustic solitary waves. Phys Plasmas 2007;14:052305. http://dx.doi.org/10.1063/1.2732176.

[21] Lakhina GS, Singh SV, Kakad AP, Goldstein ML, Vin˜as AF, Pickett JS. A mechanism for electrostatic solitary structures in the earth's magnetosheath. J Geophys Res 2009;114:A09212. http://dx.doi.org/10.1029/2009JA014306.

[22] Rufai OR, Bharuthram R, Singh SV, Lakhina GS. Low frequency solitons and double layers in a magnetized plasma with two temperature electrons. Phys Plasmas 2012;19:122308. http://dx.doi.org/10.1063/1.4771574.

[23] Rufai OR, Bharuthram R, Singh SV, Lakhina GS. Effect of hot ion temperature on obliquely propagating ion-acoustic solitons and double layers in an auroral plasma. Commun Nonlinear Sci Numer Simul 2014;19:1338–46. http://dx.doi.org/10.1016/j.cnsns.2013.09.024.

[24] Rufai OR, Bharuthram R, Singh SV, Lakhina GS. Obliquely propagating ion-acoustic solitons and supersolitons in four-component auroral plasmas. Adv Space Res 2016;57(3):813–20. http://dx.doi.org/10.1016/j.asr.2015.11.021.

[25] Rufai OR, Bharuthram R. Electrostatic fluctuations in a magnetized two-component plasma with q-nonextensive electrons and thermal ions. Phys Plasmas 2016;23:092306. http://dx.doi.org/10.1063/1.4963773.

[26] Rufai OR, Bharuthram R. Obliquely propagating low-frequency magnetospheric electrostatic solitary waves in the presence of an oxygen-ion beam. Commun Nonlinear Sci Numer Simul 2019;68:160. http://dx.doi.org/10.1016/j.cnsns.2018.08.006.

[27] Rufai OR, Bharuthram R, Maharaj SK. The effects of superthermal particles on the existence domain of oblique low-frequency solitary waves in multi-component magnetospheric plasmas. Phys Plasmas 2021;28:052901. http://dx.doi.org/10.1063/5.0031330.

[28] Singh N, Khazanov G. Double layers in expanding plasmas and their relevance to the auroral plasma processes. J Geophys Res 2003;108(A4):8007. http://dx.doi.org/10.1029/2002JA009436.

[29] Devanandhan S, Singh GS, Bharuthram R. Electron-acoustic solitons in the presence of an electron beam and superthermal electrons. Nonlnear Processes Geophys 2011;18:627–34. http://dx.doi.org/10.5194/npg-18-627-2011.

[30] Devanandhan S, Singh SV, Lakhina R. Small amplitude electron acoustic solitary waves in a magnetized superthermal plasma. Commun Nonlinear Sci Numer Simul 2015;22(1–3):1322–30. http://dx.doi.org/10.1016/j.cnsns.2014.07.026.

[31] Kakad A, Kakad B, Anekallu C, Lakhina G, Omura Y, Fazakerley A. Slow electrostatic solitary waves in the earth's plasma sheet boundary layer. J.Geophys Res: Space Physics 2016;121:4452–65. http://dx.doi.org/10.1002/2016JA022365.

[32] Lakhina GS, Singh SV, Kakad AP, Verheest F, Bharuthram R. Study of nonlinear ion- and electron-acoustic waves in multi-component space plasmas. Nonlinear Processes Geophys 2008;15:903–13. http://dx.doi.org/10.5194/npg-15-903-2008.

[33] Lakhina GS, Singh SV, Kakad AP. Ion-and electron-acoustic solitons and double layers in multi-component space plasmas. Adv Space Res 2011;47:1558–67. http://dx.doi.org/10.1016/j.asr.2010.12.013.

[34] Lotekar A, Kakad A, Kakad B. Formation of asymmetric electron acoustic double layers in the earth's inner magnetosphere. J Geophys Res: Space Phys 2019;124:6896–905. http://dx.doi.org/10.1029/2018JA026303.

[35] Mbuli LN, Maharaj SK, Bharuthram R, Singh SV, Lakhina GS. Arbitrary amplitude slow electron-acoustic and ion-acoustic solitons in three-electron temperature space plasmas. Phys Plasmas 2015;22:062307. http://dx.doi.org/10.1063/1.4922683.

[36] Mbuli LN, Maharaj SK, Bharuthram R, Singh SV, Lakhina GS. Arbitrary amplitude fast electron-acoustic solitons in three-electron component space plasmas. Phys Plasmas 2016;23(6):062302. http://dx.doi.org/10.1063/1.4952637.

[37] Rubia R, Singh SV, Lakhina GS. Existence domain of electrostatic solitary waves in the lunar wake. Phys Plasmas 2018;25:032302. http://dx.doi.org/10.1063/1.5017638.

[38] Singh SV, Reddy RV, Lakhina GS. Broadband electrostatic noise due to nonlinear electron-acoustic waves. Adv Space Res 2001;28(11):1643–8.

[39] Singh SV, Devanandhan S, Lakhina GS, Bharuthram R. Electron acoustic solitary waves in a magnetized plasma with nonthermal electrons and an electron beam. Phys Plasmas 2016;23:082310. http://dx.doi.org/10.1063/1.4961961.

[40] Vasko IY, Agapitov OV, Mozer FS, Bonnell JW, Artemyev AV, Krasnoselskikh VV, et al. Electron-acoustic solitons and double-layers in the inner magnetosphere. Geophys Res Lett 2017;44:4575–83. http://dx.doi.org/10.1002/2017GL074026.

[41] Vasko IY, Agapitov OV, Mozer FS, Bonnell JW, Artemyev AV, Krasnoselskikh VV, et al. Electrostatic steepening of whistler waves. Phys Rev Lett 2018;120:195101. http://dx.doi.org/10.1103/PhysRevLett.120.195101.

[42] Dillard CS, Vasko IY, Mozer FS, Agapitor OV, Bonnel JW. Electron-acoustic solitary waves in the earth inner magnetosphere. Phys Plasmas 2018;25:022905. http://dx.doi.org/10.1063/1.5007907.

[43] Argall MR, Paulson K, Alm L, Rager A, Dorelli J, Shuster J, et al. Electron dynamics within the electron diffusion region of asymmetric reconnection. J Geophys Res: Space Phys 2018;123:146–62. http://dx.doi.org/10.1002/2017JA024524.

[44] Bessho N, Chen L-J, Hesse M. Electron distribution functions in the diffusion region of asymmetric magnetic reconnection. Geophys Res Lett 2016;43:1828–36. http://dx.doi.org/10.1002/2016GL067886.

[45] Burch JL, Torbert RB, Phan TD, Chen L-J, Moore TE, Ergun RE, et al. Electron-scale measurements of magnetic reconnection in space. Science 2016;352:6290. http://dx.doi.org/10.1126/science.aaf2939.

[46] Chen L-J, Wang S, Hesse M, Ergun RE, Moore T, Giles B, et al. Electron diffusion regions in magnetotail reconnection under varying guide fields. Geophys Res Lett 2019;46:6230–8. http://dx.doi.org/10.1029/2019GL082393.

[47] Hwang K-J, Choi E, Dokgo K, Burch JL, Sibeck DG, Giles BL, et al. Electron vorticity indicative of the electron diffusion region of magnetic reconnection. Geophys Res Lett 2019;46:6287–96. http://dx.doi.org/10.1029/2019GL082710.

[48] Nakamura R, Genestreti KJ, Nakamura T, Baumjohann W, Varsani A, Nagai T, et al. Structure of the current sheet in the 11 2017 electron diffusion region event. J Geophys Res: Space Physics 2019;124:1173–86. http://dx.doi.org/10.1029/2018JA025713.

[49] Torbert RB, Burch JL, Phan TD, Hesse M, Argall MR, Shuster J, et al. Electron-scale dynamics of the diffusion region during symmetric magnetic reconnection in space. Science 2018;362:1391–5, https://science.sciencemag.org/content/sci/362/6421/1391.full.pdf.

[50] Schamel H. Theory of electron holes. Phys Scr 1979;20:336–42. http://dx.doi.org/10.1088/0031-8949/20/3-4/006/pdf.

[51] Williams G, Verheest F, Hellberg MA, Anowar MGM, Kourakis I. A schamel equation for ion acoustic waves in superthermal plasmas. Phys Plasmas 2014;21:092103. http://dx.doi.org/10.1063/1.4894115.

[52] Abbasi H, Hakimi Pajouh H. Influence of trapped electrons on ion-acoustic solitons in plasmas with superthermal electrons. Phys Plasmas 2007;14:012307. http://dx.doi.org/10.1063/1.2428281.

[53] Mamun AA, Cairns RA, Shukla PK. Effects of vortex-like and non-thermal ion distributions on non-linear dust-acoustic waves. Phys Plasmas 1996;3:2610. http://dx.doi.org/10.1063/1.871973.

[54] Mamun AA, Shukla PK. Electron-acoustic solitary waves via vortex electron distribution. J Geophys Res 2002;107(A7):1135. http://dx.doi.org/10.1029/2001JA009131.

[55] Mamun AA, Shukla PK, Stenflo L. Obliquely propagating electron-acoustic solitary waves. Phys Plasmas 2002;9(4):1474–7. http://dx.doi.org/10.1063/1.1462635.

[56] Mushtaq A, Ikram M, Clark REH. Electrostatic solitary waves in pair-ion plasmas with trapped electrons. Braz J Phys 2014;44:614–21. http://dx.doi.org/10.1007/s13538-0261-3.

[57] Rufai OR, Khazanov GV, Singh SV. Finite amplitude electron-acoustic waves in the electron diffusion region. Results Phys 2021;24:104041. http://dx.doi.org/10.1016/j.rinp.2021.104041.

[58] Singh SV, Lakhina GS, Bharuthram R, Pillay SR. Electrostatic solitary structures in presence of non-thermal electrons and a warm electron beam on the auroral field lines. Phys Plasmas 2011;18:122306. http://dx.doi.org/10.1063/1.3671955.